Sharp-line Electronic Spectroscopy and Ligand Field Analysis of Cr(III) Complexes with Amino Acid Ligands

Sung-Jin Park, Young-Keun Choi, Seung-Suk Han, and Kyu-Wang Lee*

Department of Chemistry and Electronic Materials Research Center, Myongji University, Yongin, Kyonggi-Do 449-728, Korea
Received July 15, 1999

Ligand field calculations have been performed based on the data from the absorption and low temperature sharp-line excitation spectra of *fac*-Cr(gly)$_3$, *fac*-Cr(L-serine)$_3 \cdot 2H_2O$ and *fac*-Cr(L-leucine)$_3 \cdot 2H_2O$. The optimized ligand field parameters for all complexes show that the carboxylate and the amino groups are moderate σ-donor. The values of $e_{\pi O}$ are typical of other complexes with carboxylate ligands. However, the π-interaction of carboxylic oxygen to the chromium in serinato complex is much weaker than that of other complexes. The inclusion of π-anisotropy is necessary to adequately explain the large doublet splittings.

Introduction

Transition metal complexes with amino acids have been studied extensively as a model for metal center in biological system.[1-3] In particular, chromium(III) complexes are quite useful for this purpose since they are so kinetically inert that various complexes could be isolated and show three spin allowed transition bands and a number of clearly defined spin forbidden transitions. The studies have been based primarily on UV-visible absorption and circular dichroism spectroscopy.[4-6]

Sharp-lines are frequently observed in the electronic spectra of the chromium(III) complexes. These arises when an electron undergoes a spin flop or hop within the t_{2g} shell and they are very sensitive to the small perturbation like metal-ligand geometry or spin-orbit coupling. Also these convey most of the π-bonding information and the sharp-line electronic spectroscopy has been a primary tool for finer detailed analysis of ligand field theory.[7-8]

In this paper, we analyzed the sharp-line electronic spectra of the chromium(III) complexes with amino acids of glycine, serine and leucine in the framework of the angular overlap model (AOM) to determine the ligand field properties of the amine and carboxylate groups in the amino acids. In case of Cr(III) glycine complex, the ligand field parameters which were previously determined from the isotropic π bonding formalism are reinvestigated. With this formalism, the quantitative σ and π contributions of each ligand can be estimated by consideration of the each individual ligand geometry.

Experimental Section

The free ligand L-serine and L-leucine were used as obtained from Aldrich. *fac*-Cr(L-serine)$_3 \cdot 2H_2O$ was synthesized according to the method of Mizuochi *et al.*[9] L-serine was added to a solution of chromium(III) chloride hexahydrate. After the reaction under basic conditions, pink crystals were obtained. To prepare *fac*-Cr(L-leucine)$_3 \cdot 2H_2O$, hexaamminechromium(III) nitrate was mixed with L-leucine.[10-11] The reaction product was dissolved in ethanol and the residues were removed by filtration. Pink crystals were recrystallized twice.

A Continuum Nd:YAG laser-pumped dye laser (ND60) was used as a excitation source in the luminescence and excitation spectroscopy. The emission was measured with a CVI 0.5 m monochromator (DK 480) and a cooled photomultiplier (Hamamatsu R943-02). A SRS boxcar averager was used for signal processing. Microcrystalline samples were mounted with conductive grease on the cold head of a Janis CCS-600 closed-cycle He gas cryostat. Infrared spectra were measured with a Perkin-Elmer System 2000 FTIR spectrometer on samples dispersed in Nujol mulls on a polyethylene film (far-IR) or in KBr pellets (mid-IR). Room temperature absorption spectra were recorded with a Shimadzu UV 3100 spectrophotometer.

Results and Discussion

Luminescence Spectrum. Figure 1 shows the 12K luminescence spectra of *fac*-Cr(L-serine)$_3 \cdot 2H_2O$ and *fac*-Cr(L-leucine)$_3 \cdot 2H_2O$. The zero phonon lines appear to be very

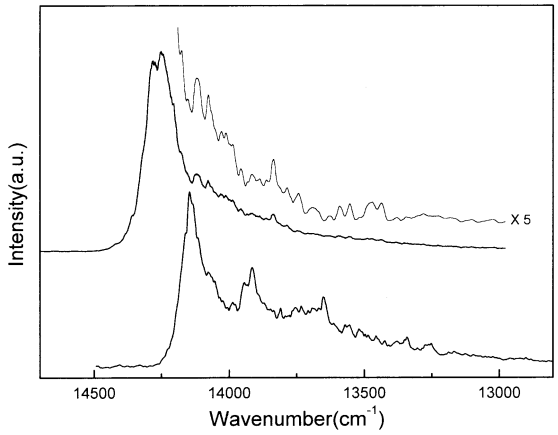

Figure 1. Luminescence spectra of *fac*-Cr(L-serine)$_3$ and *fac*-Cr(L-leucine)$_3$ at 12 K. lower: *fac*-Cr(L-serine)$_3$, upper: *fac*-Cr(L-leucine)$_3$.

Table 1. Vibronic intervals in the 12 K luminescence spectrum of Cr(L-serine)$_3$ and Cr(L-leucine)$_3$. (all data in cm^{-1})

Cr(L-serine)$_3$		Cr(L-leucine)$_3$		Assignment
Lumin.	IR	Lumin.	IR	
14				
32				
51	55	46	45	Lattice
70	76	75	69, 85	
		132	133	
160	156	172	166, 184	N-Cr-O
201	207	222	221	Bending
232	243	238	238	
	262		265, 272	C-C-C bending
	285		296	N-H torsion
	321		321	C-C-N bending
337	340	335	348	Cr-O Stretching
	371		367	C-C-N bending
393	403	387	400	Cr-O Stretching
412	420	413		Cr-N Stretching
455	445	465	442	Cr-N Stretching
496	492			
	527		538	C-C-O bending
574	562, 571			
590	588			
628	621		621	
689	683		683	
721				
766				
804	810			
843	834			
885	872			

strong indicating that the symmetry of both complexes is very low. Peaks are rather broad and the vibrational structures for both complexes are quite weak. The spectra obtained were independent of the exciting wavelength within the first spin allowed band. No evidence for impurity was observed in other analytical methods. Since dehydration of both samples was observed during the spectroscopic measurement, the broadness of the spectra are probably due to the inequivalent sites in crystals.

The vibronic intervals and their assignments for *fac*-Cr(L-serine)$_3$ and *fac*-Cr(L-leucine)$_3$ are listed in Table 1 along with far-IR data. The luminescence spectrum of *fac*-Cr(L-serine)$_3$ shows large number of vibrational peaks, though they are weak. The peaks below 300 cm^{-1} correspond to ring deformations with considerable δ(N-Cr-O) and carboxylate bending character. The vibrational modes were assigned based on the large body of vibrational data of metal-amino acid complexes.[12] The 262, 285, 321, 371 cm^{-1} bands in far-IR spectrum can be assigned to C-C-C bending, N-H torsion and two C-C-N bending modes of amino acid skeleton, respectively (Figure 2). The Cr-O stretching modes are observed at 337 cm^{-1} and 393 cm^{-1} in luminescence and also comparable to two Cr-O IR modes (340, 403 cm^{-1}). The bands at 412 and 455 cm^{-1} are assigned to the Cr-N stretching frequencies. Since the symmetry of the complex is low and the spectral resolution is rather poor, the identification of

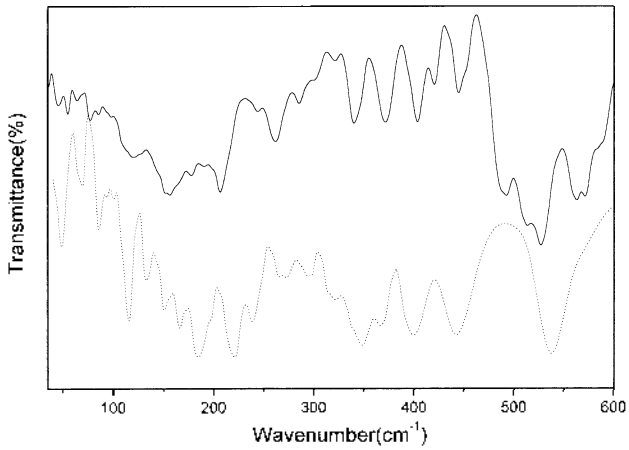

Figure 2. Far-IR spectra of *fac*-Cr(L-serine)$_3$ and *fac*-Cr(L-leucine)$_3$. *fac*-Cr(L-serine)$_3$: solid line, *fac*-Cr(L-leucine)$_3$: dotted line.

these stretching modes to symmetric and asymmetric one is difficult. The weak bands appeared up to 900 cm^{-1} in the luminescence spectrum have counter part in the IR spectrum and the existence of combination band is not apparent.

The vibrational structure of *fac*-Cr(L-leucine)$_3 \cdot 2H_2O$ is similar to that of serinato complex, especially in coordination sphere, since the vibrational frequencies of Cr-ligands modes are similar to each other, as seen in Table 1.

Excitation Spectrum. The 12 K excitation spectra of *fac*-Cr(L-serine)$_3 \cdot 2H_2O$ and *fac*-Cr(L-leucine)$_3 \cdot 2H_2O$ in the doublet region are shown in Figure 3 and Figure 4, respectively. The peak positions and assignments are tabulated in Table 2. The lowest energy peak at 14192 cm^{-1} in excitation spectrum of *fac*-Cr(L-serine)$_3 \cdot 2H_2O$ coincide with the emission origin and is assigned to the lower component of the $^4A_{2g} \rightarrow {}^2E_g$ transition. The second component can be assigned to the relatively strong peak at 14499 cm^{-1}. The splitting by 307 cm^{-1} is quite large compared to the other Cr(III) complexes with amino acid ligands, such as glycine, histidine and glycylglycine.[13-15] The three components of $^2T_{1g}$ transition peaks are located at 14876, 15176 and 15264 cm^{-1}. Though these peaks are rather weak, vibronic bands based

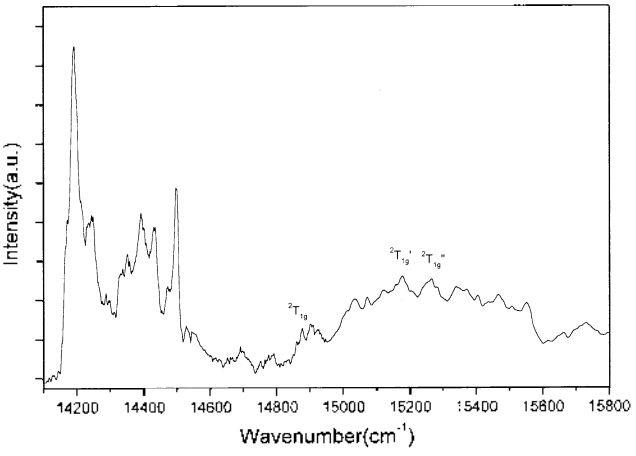

Figure 3. 12 K Excitation spectrum of *fac*-Cr(L-serine)$_3$ in the region of ^2E_g, $^2T_{1g}$ excited states.

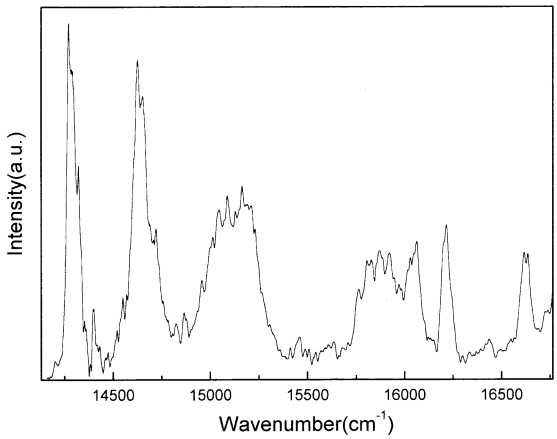

Figure 4. 12 K Excitation spectrum of *fac*-Cr(L-leucine)$_3$ in the region of ^2E_g, $^2T_{1g}$ excited states.

Table 2. Peak positions in the 12 K excitation spectrum of Cr(L-serine)$_3$. (all data in cm^{-1})

$\bar{\nu}$ - 14192	Assignment	$\bar{\nu}$ - 14192	Assignment
0 vs	^2E_g	717 w	^2E_g' + 412
42 w		731 vw	$^2T_{1g}$ + 52
52 w	^2E_g − 52	808 sh	^2E_g' + 496
95 vw		817 sh	
104 vw		841 w	^2E_g + 843, $^2T_{1g}$ + 160
159 w	^2E_g + 160	879 w	^2E_g + 884, $^2T_{1g}$ + 201
200 m	^2E_g + 201	927 vw	$^2T_{1g}$ + 232
240 m	^2E_g + 232	984 w	$^2T_{1g}$'
280 vw		1012 vw	$^2T_{1g}$ + 337
307 s	^2E_g'	1072 w	$^2T_{1g}$"
336 vw	^2E_g + 337	1088 vw	$^2T_{1g}$ + 412
356 vw	^2E_g' + 52	1147 w	^2E_g' − 843, $^2T_{1g}$' + 160
391 vw	^2E_g+ 393	1179 vw	$^2T_{1g}$ + 496, $^2T_{1g}$' − 201
409 vw	^2E_g + 412	1212 w	$^2T_{1g}$' + 232
460 vw	^2E_g' + 160	1241 w	$^2T_{1g}$" + 160
498 vw	^2E_g + 496	1273 w	$^2T_{1g}$ + 590, $^2T_{1g}$" − 201
509 vw	^2E_g' + 201	1314 vw	$^2T_{1g}$" + 232
583 vw	^2E_g' + 387	1358 w	
598 vw		1421 vw	
642 vw	^2E_g' + 337	1470 vw	$^2T_{1g}$' + 496, $^2T_{1g}$" + 393
657 vw		1538 w	
684 w	$^2T_{1g}$	1573 w	$^2T_{1g}$' + 590, $^2T_{1g}$" + 496
708 w	^2E_g' + 393	1574 vw	$^2T_{1g}$" + 590

on these origins are similar in frequency and intensity pattern to those based on ^2E_g electronic origins.

The five lowest doublet electronic origins of *fac*-Cr(L-leucine)$_3 \cdot 2H_2O$ are identified by using the same method and tabulated in Table 3. The ^2E_g splitting of 353 cm^{-1} is even lager than that of serinato complex.

The spin-allowed transitions to the $^4T_{2g}$ and $^4T_{1g}$ excited states were observed in the solution absorption spectrum at room temperature. Since the $^2T_{2g}$ bands are so weak and are sandwiched between much stronger quartet bands, $^4T_{2g}$ and $^4T_{1g}$, their identification with the excitation or the absorption spectra was not successful. The second derivative of the absorption spectra show the sharp line structure at 21891 and 22382 cm^{-1} for *fac*-Cr(L-serine)$_3 \cdot 2H_2O$ and *fac*-Cr(L-leucine)$_3 \cdot 2H_2O$, respectively. These are assigned to the first

Table 3. Peak positions in the 12 K excitation spectrum of Cr(L-leucine)$_3$. (all data in cm^{-1})

$\bar{\nu}$ - 14271	Assignment	$\bar{\nu}$ - 14271	Assignment
0 s	^2E_g	1188 w	$^2T_{1g}$ + 295
20 sh		1216 vw	
51 w	^2E_g − 47	1236 vw	$^2T_{1g}$ + 336
81 vw	^2E_g − 75	1271 vw	$^2T_{1g}$ + 388
127 w	^2E_g + 133	1298 vw	$^2T_{1g}$ + 414
159 vw		1321 vw	
189 vw		1336 vw	
202 vw		1365 vw	$^2T_{1g}$ + 466
249 vw	^2E_g + 239	1410 vw	
279 vw		1436 vw	
298 vw	^2E_g + 295	1490 w	
353 s	^2E_g'	1535 w	
380 w	^2E_g + 388	1556 w	
418 vw	^2E_g + 414	1599 w	
436 vw	^2E_g' + 75	1650 w	$^2T_{1g}$'
450 w	^2E_g + 466	1698 vw	$^2T_{1g}$' − 47
486 vw	^2E_g' − 133	1746 w	
552 vw		1758 w	
593 w	^2E_g' − 239	1789 m	$^2T_{1g}$"
684 w	^2E_g' − 336	1877 vw	$^2T_{1g}$' + 239
741 sh	^2E_g' − 388	1928 sh	$^2T_{1g}$" + 133
773 w	^2E_g' − 414	1944 m	
815 w	^2E_g' − 466	2028 vw	$^2T_{1g}$' + 388, $^2T_{1g}$" + 239
858 vw		2062 vw	
892 w	$^2T_{1g}$	2120 vw	$^2T_{1g}$" + 336
919 vw		2146 vw	$^2T_{1g}$' + 272
939 vw		2163 vw	$^2T_{1g}$" + 388
960 vw	$^2T_{1g}$ − 75	2222 vw	
1035 sh	$^2T_{1g}$ + 133	2343 w	
1141 vw	$^2T_{1g}$ + 239	2364 w	

component of the $^2T_{2g}$ transition, but the spectrums are not resolved well enough to assign other components with any certainty.

Ligand Field Analysis. The general methods to determine the eigenvalues and eigenfunctions of a d^3 ion in the ligand field have been described elsewhere.[14-16] Transition energies were obtained by diagonalization of the full 120 × 120 secular determinant, which was developed by means of a Hamiltonian including interelectronic repulsion with a Trees correction, spin-orbit coupling and the ligand field potential expressed in the angular overlap model (AOM) formalism through the σ- and π-interaction. The ligand field potential matrix was generated only from the six coordinated atoms by use of the X-ray single crystal structure,[17] as described previously.[7] Since crystal structures for *fac*-Cr(L-serine)$_3 \cdot 2H_2O$ and *fac*-Cr(L-leucine)$_3 \cdot 2H_2O$ are not available, their structure were obtained from molecular mechanic (MM2) calculation.[18]

The nine parameters varied during the optimization were the AOM ligand field parameters $e_{\sigma O}$ and $e_{\pi O}$ for carboxylate oxygen, $e_{\sigma N}$ for the amine nitrogen, plus the interelectronic repulsion parameters B, C and α_T (the Trees correction parameter), and the spin-orbit coupling parameter ζ. The amine nitrogen was assumed to have no π-bonding capability. The π-interaction of the carboxylate oxygen with the metal ion

was considered to be anisotropic. The anisotropy of metal-ligand π-interaction can be expressed by parallel ($e_{\pi c}$) and perpendicular ($e_{\pi s}$) parameters. To avoid a knotty problem in proper partitioning between two parameters, however, the π-interaction of the ligand was expressed entirely through $e_{\pi s}$ by rotation of coordinates through the π orientation angle ψ, and the value of $e_{\pi c}$ was set to zero.[7,14]

The experimental transition energies used in the fitting procedure, along with their assignment in O_h notation, are included in Table 4. By variation of the nine parameters just described, these energies were fit by means of the Powell parallel subspace optimization procedure.[19] The function minimized was

$$F = \sum Q^2 + 10\sum T^2 + 100\sum D^2 + 1000\sum S^2$$

where each term represents a difference between experimental and calculated transition energies or splittings: D, the five lowest doublet energies; T the averaged $^2T_{2g}$ peak position; Q, the two quartet energies and S, the splittings between the doublet energies. The weighting factors in this function are in approximate proportion to the inverse square of the corresponding experimental uncertainty. All parameters were constrained to reasonable limits based on the data from other Cr(III) complexes, but none of them approached to the boundaries in the best-fit parameter set. The optimization was repeated several times with different sets of starting parameters to confirm that the same global minimum was found.

The result of the optimization and the parameter set used to generate the best-fit energies of $Cr(gly)_3$, $Cr(L\text{-serine})_3 \cdot 2H_2O$ and $Cr(L\text{-leucine})_3 \cdot 2H_2O$ are listed in Table 4. The optimized ligand field parameters of all complexes show that the carboxylate and the amino groups are moderate σ-donor. The values of $e_{\pi O}$ are typical of other complexes with carboxylate ligands. However, the π-interaction of carboxylic oxygen to the chromium in serinato complex is much weaker than that of other complexes.

The ligand field strength, Δ or 10 Dq, can be estimated roughly for each ligand by the relationship of $\Delta = 3e_\sigma - 2e_\pi$ for nonlinear, anisotropic π ligands. The ligand field parameters from the best-fit parameter set yield the Δ values

Table 4. Experimental and calculated transition energies for Cr(L-serine)$_3$, Cr(L-leucine)$_3$ and *fac*-Cr(glycine)$_3$ complex. (all data in cm^{-1})

	Cr(L-serine)$_3$		Cr(L-leucine)$_3$		*fac*-Cr(gly)$_3$		
	Obs.	Calc.[a]	Obs.	Calc.[b]	Obs.[12]	Calc.[c]	Calc.[d]
^2E_g	14192	14182	14271	14303	14485	14471	14465
	14499	14521	14624	14623	14579	14569	14604
$^2T_{1g}$	14876	14833	15163	15311	14842	15031	14999
	15176	15105	15921	15863	15350	15229	15248
	15264	15276	16060	15962	15442	15400	15361
$^2T_{2g}$	21891	21875	22382	22410			
$^4T_{2g}$(avg)	18790	18781	19305	18853	19880	19695	19713
$^4T_{1g}$(avg)	25138	25147	25458	25608	26040	25147	26192

[a]ligand field parameters: $e_{\sigma O}$ = 7401, $e_{\pi O}$ = 639, $e_{\sigma N}$ = 6621, B = 671, C = 2917, T= 133, ζ = 24. [b]$e_{\sigma O}$ = 7116, $e_{\pi O}$ = 1242, $e_{\sigma N}$ = 6751, B = 787, C = 2639, T = 250, ζ = 271. [c]$e_{\sigma O}$ = 8832, $e_{\pi O}$ = 2000, $e_{\sigma N}$ = 6843.B = 805, C = 2833, ζ = 266, isotropic π interaction. Ref.12. [d]$e_{\sigma O}$ = 7283, $e_{\pi O}$ = 1513, $e_{\sigma N}$ = 7240, B = 657, C = 3090, T = 69, ζ = 10, anisotropic π interaction.

fac-Cr(L-serine)$_3$: Δ_N = 19863 cm^{-1} , Δ_O = 20925 cm^{-1}
fac-Cr(L-leucine)$_3$: Δ_N = 20253 cm^{-1} , Δ_O = 18864 cm^{-1}
fac-Cr(L-glycine)$_3$: Δ_N = 21720 cm^{-1} , Δ_O = 18823 cm^{-1}

The ligand field strength of amine nitrogen and carboxylate oxygen is reversed in Cr(L-serine)$_3$, but the ligand field strength of each ligand remains in similar magnitudes. All of the other parameters are reasonable in comparison with other Cr(III) complexes. Large variance of spin-orbit coupling parameter, ζ, gives no significance because the splittings of doublet transition lines are too large to be explained by spin-orbit coupling.

It is worth to mention the significance of anisotropic π-interaction in a ligand field analysis. The orientation of the π-orbital in a nonlinear ligand affects the metal d orbital energies significantly. The ligand field analysis of *fac*-Cr(L-glycine)$_3$ with isotropic π-bonding yielded the e_σ and e_π values of 8832 and 2000 cm^{-1} and the overall fittings were rather poor.[12] These values seemed too high compared to the other carboxylate oxygens and they are comparable to the oxide ion as observed in the ruby spectrum.[20] The inclusion of anisotropic π-bonding in ligand field analysis of *fac*-Cr(gly)$_3$ markedly improve the overall fittings and the optimized ligand field parameters are in a reasonable range, as seen in Table 4.

References

1. Green, C.; Place, H.; Willet, R. D.; Legg, J. I. *Inorg.Chem.* **1986**, *25*, 4672.
2. El-Shahawi, M. S. *Transition Met. Chem.* **1993**, *18*, 385.
3. Djordjevic, C.; Vuletic, N.; Jacobs, B. A.; Leerensio, M. *Inorg. Chem.* **1997**, *36*, 1798.
4. Kazaki, S.; Ito, M. *Bull. Chem. Soc. Jpn.* **1981**, *54*, 2499.
5. Tsubomura, T.; Ohkouchi, I.; Morita, M. *Bull. Chem. Soc. Jpn.* **1991**, *64*, 2341.
6. Pedrosa, J.; Jesus, D.; DosSantos, T. M. *Polyhedron* **1991**, *10*(6), 575.
7. Hoggard, P. E. *Coord. Chem. Rev.* **1986**, *70*, 85.
8. Schönherr, T. *Topics in Curr. Chem.* **1997**, *191*, 87.
9. Mizuochi, H.; Uchara, A.; Kyuno, E.; Tsuchiya, R. *Bull. Chem. Soc. Jpn.* **1971**, *44*, 1555.
10. Oki, H.; Otsuka, K. *Bull. Chem. Soc. Jpn.* **1976**, *49*(7), 1841.
11. Oki, H. *Bull. Chem. Soc. Jpn.* **1977**, *50*(3), 680.
12. Nakamoto, K. *Infrared and Raman Spectra of Inorganic and Coordination Compounds*, 5th ed.; John Willy & Sons, Inc.; 1997.
13. Wallace, W. M.; Hoggard, P. E. *Inorg. Chem.* **1983**, *22*, 491.
14. Lee, K. W.; Eom, K. I.; Park, S. J. *Inorg. Chim. Acta* **1997**, *254*, 131.
15. Subramanam, V.; Lee, K. W.; Garvey, R. G.; Hoggard, P. E. *Polyhedron* **1988**, *7*(7), 523.
16. Park, S. J.; Lee, K. W. *Chem. Phys.* **1996**, *202*, 15.
17. Bryan, R. F.; Greene, P. T.; Stokley, P. F.; Wilson, E. W. *Inorg. Chem.* **1971**, *10*(7), 1468.
18. Burkert, U.; Allinger, N. L. Molecular Mechanics; *ACS Monograph* 177; American Chemical Society: Washington, DC, 1982.
19. Powell, M. J. D. *Comput. J.* **1964**, *7*, 155.
20. Lee, K. W.; Hoggard, P. E. *Inorg. Chem.* **1990**, *28*, 850.